SYNTHESIS AND CHARACTERIZATION OF Ag/BiOBr NANOCOMPOSITES FOR PHOTODEGRADATION OF METHYLENE BLUE AS MODEL DYE

A. PHURUANGRAT[a,*], K. RABIABDEE[a], S. THONGTEM[b,c], T. THONGTEM[c,d]
[a]*Department of Materials Science and Technology, Faculty of Science, Prince of Songkla University, Hat Yai, Songkhla 90112, Thailand*
[b]*Department of Physics and Materials Science, Faculty of Science, Chiang Mai University, Chiang Mai 50200, Thailand*
[c]*Materials Science Research Center, Faculty of Science, Chiang Mai University, Chiang Mai 50200, Thailand*
[d]*Department of Chemistry, Faculty of Science, Chiang Mai University, Chiang Mai 50200, Thailand*

Ag/BiOBr nanocomposites with different Ag contents were prepared by deposition-sonochemical method. Phase and morphology of the products were investigated by X-ray diffraction (XRD), scanning electron microscopy (SEM), transmission electron microscopy (TEM) and X-ray photoelectron spectroscopy (XPS). The experimental results showed that Ag nanoparticles supported on surface of tetragonal BiOBr nanoplates. The photocatalytic properties of Ag/BiOBr nanocomposites were investigated through photocatalytic degradation of methylene blue (MB) under UV light irradiation. In this research, 10 wt% Ag/BiOBr nanocomposites showed the highest photocatalytic activity under visible light irradiation.

(Received November 28, 2018; Accepted April 18, 2019)

Keywords: Ag/BiOBr nanocomposites; Photocatalysis; X-ray diffraction; Spectroscopy

1. Introduction

Due to the increase of industrialization and urbanization, the environmental problem and the energy crisis have become the subject of great interest to worldwide researchers [1, 2]. Bi-based photocatalysts have attracted much attention owing to the excellent photocatalytic activity of organic compounds and water splitting [1, 3]. Among them, BiOBr with narrow band gap of 2.75 eV has proved to be an efficient visible light photocatalyst for environmental treatment due to its layered tetragonal matlockite structure, a layered structure made up of [Br–Bi–O–Bi–Br] slabs stacked together by van der Waals attraction. In this pattern, each Bi center is surrounded by four O atoms and four Br atoms, leading to asymmetric decahedral symmetry [1, 4-6]. This structure is a very important pattern for photocatalytic reaction. It can provide large enough space to polarize the related atoms and orbitals and promote the separation of electrons and holes [4, 6, 7]. Moreover, a quick recombination of photogenerated charge carriers still exists in BiOBr to restrain its photocatalytic activity [1]. To solve this problem, noble metal nanoparticles are deposited on BiOBr in order to enhance the photocatalytic activity of BiOBr [7, 8]. This efficient and promising material acts as a reservoir for photogenerated electrons, promoting the interfacial electron diffusion process and facilitating photocatalytic reaction [7, 8].

In this work, a series of Ag/BiOBr nanocomposites with different weight ratios of Ag on BiOBr nanoplates was synthesized by a sonochemical method. The results showed that the as-synthesized Ag/BiOBr nanocomposites exhibited higher photocatalytic activity for photodegradation of methylene blue (MB) under UV light irradiation than pure BiOBr.

* Corresponding authors: phuruangrat@hotmail.com

2. Experiment

In a typical hydrothermal synthesis, each of $Bi(NO_3)_3 \cdot 5H_2O$ and NaBr was dissolved in 100 ml deionized water, stirred for 30 min and mixed together. Then 25 ml 3 M NaOH were added to the mixed solution. The suspension was transferred to a 200 ml Teflon-lined autoclave and heated at 180 ^oC for 20 h. The as-synthesized precipitates were filtered, thoroughly washed and dried for further characterization.

To prepare 1–10 wt% Ag/BiOBr nanocomposites, different weight contents of $AgNO_3$ were dissolved in 2.5 g BiOBr suspension containing in 100 ml ethylene glycol which was vibrated by ultrasonic radiation for 30 min. The as-prepared precipitates were collected, washed with deionized water three times and dried at 80 ^oC for 24 h for further characterization.

X-ray powder diffraction patterns were obtained by an X-ray diffractometer (XRD, Philips X'Pert MPD X-ray diffractometer) with CuK_α radiation (λ=1.5406 Å) as an X-ray source. The morphologies of materials were obtained by using a scanning electron microscope (SEM) with a JEOL model JSM 6335F operating at 35 kV and a transmission electron microscope (TEM JEOL model JEM 2010) employing at an accelerating voltage of 200 kV. X-ray photoelectron spectroscopy (XPS) of the products was carried out by a Kratos X-ray photoelectron spectrometer (Axis Ultra DLD, Kratos Analytical Ltd) with a monochromated Al K_α (1486.6 eV) radiation as an excitation source. All obtained spectra were calibrated to a C 1*s* electron peak at 285.1 eV.

Photocatalytic activity was evaluated through the degradation of MB solution. The 0.2 g photocatalyst was added to $1x10^{-5}$ M of 200 ml MB solution which was magnetically stirred to form homogeneous solution. For every 60 min specific time interval, solution was withdrawn and centrifuged. The solution was measured by a Lambda 25 UV–visible spectrophotometer (Perkin Elmer) at λ_{max} of MB = 664 nm. The degradation of MB was calculated using the below equation as follows.

$$\text{Decolorization efficiency (\%)} = \frac{C_o - C_t}{C_o} x100 \quad (1)$$

, where C_o is the initial concentration of MB and C_t is the concentration of MB after UV light irradiation within the elapsed time (t).

3. Results and discussion

Phase and purity of the as-obtained products were analyzed by X-ray diffraction (XRD) as the results shown in Fig. 1. All diffraction peaks of BiOBr without being loaded with Ag were indexed to the tetragonal phase of BiOBr with lattice constant of a = b = 3.9255 Å and c = 8.1025 Å, agree well with the database of JCPDS no. 09-0393 [9].

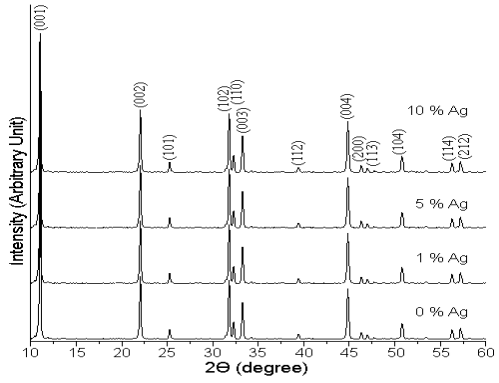

Fig. 1. XRD patterns of 0–10 wt% Ag/BiOBr samples.

The diffraction peaks were sharp, implying that the product has high crystalline degree. No peaks of impurities were detected which indicated the high purified product. Upon loading with 1–10 wt% Ag on BiOBr surface, there were no detection of metallic Ag on the samples. Possibly, Ag content was too low to be detected and Ag nanoparticles were very high dispersive on the BiOBr surface.

The morphology and microstructure of the samples were observed by SEM and TEM. SEM image of the as-prepared BiOBr sample is shown in Fig. 2a. It can be seen that the as-obtained sample consist of irregular nanoplates, in accordance with the TEM image shown in Fig. 2b. SAED pattern was studied crystalline facets of BiOBr as the result inserted in Fig. 2b, and appeared as the bright spot pattern. This analyzed pattern certified that BiOBr is very good single crystal. The SAED pattern was indexed to the (1–10) (200) and (110) planes with the [001] direction as zone axis, in agreement with those of the XRD analysis. In conclusion, the BiOBr nanoplate was surrounded by the {001} facets on the top and bottom surfaces and the {110} facets on the side surfaces [4, 5]. Fig. 2c and d shows SEM images of 5 wt% and 10 wt% Ag/BiOBr nanocomposites, respectively. They can be seen that the spherical Ag nanoparticles were deposited on the BiOBr nanoplates, suggesting that Ag/BiOBr microstructure was likely to remain unchanged after being loaded with Ag nanoparticles. The Ag nanoparticles were uniformly distributed across the BiOBr surface.

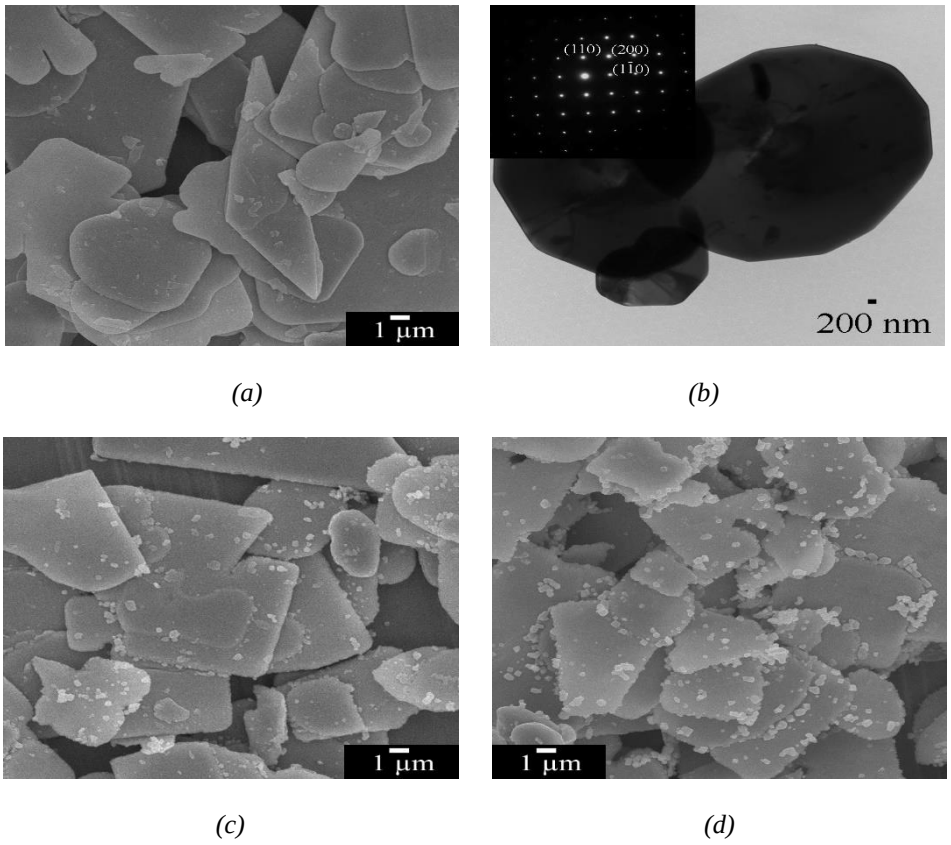

Fig. 2. SEM images, TEM image and SAED pattern of (a and b) BiOBr, (c) 5 wt% Ag/BiOBr and (d) 10 wt% Ag/BiOBr photocatalysts.

The chemical state and the interaction between Ag and BiOBr in 10 wt% Ag/BiOBr nanocomposites were investigated by XPS as the results shown in Fig. 3. The core level of Bi 4f shows two binding energy peaks at 159.40 eV and 164.74 eV, assigned to the binding energies of Bi $4f_{7/2}$ and Bi $4f_{5/2}$ containing in BiOBr [2, 5, 6, 10]. Two binding energy peaks at 68.59 eV and 69.58 eV were attributed to Br $3d_{5/2}$ and Br $3d_{3/2}$ of Br 3d core level of BiOBr [5, 6, 10]. The O 1s

binding energy of 530.47 eV was attributed to the lattice oxygen of BiOBr [5, 6, 10]. The metallic Ag of Ag/BiOBr nanocomposites shows binding energies of Ag $3d_{5/2}$ (368.12 eV) and Ag $3d_{3/2}$ (374.12 eV) [2, 11]. The 6.0 eV energy difference between these two peaks corresponds with the characteristic peak of metallic Ag, certifying the existence of Ag^0 nanoparticles [2, 11]. They should be noted that these energy peaks are less than those of the standard pure metallic Ag (Ag $3d_{5/2}$ and Ag $3d_{3/2}$ for bulk Ag are about 368.2 eV and 374.2 eV, respectively [11]), due to the interaction of Ag nanoparticles and BiOBr nanoplates of the nanocomposites.

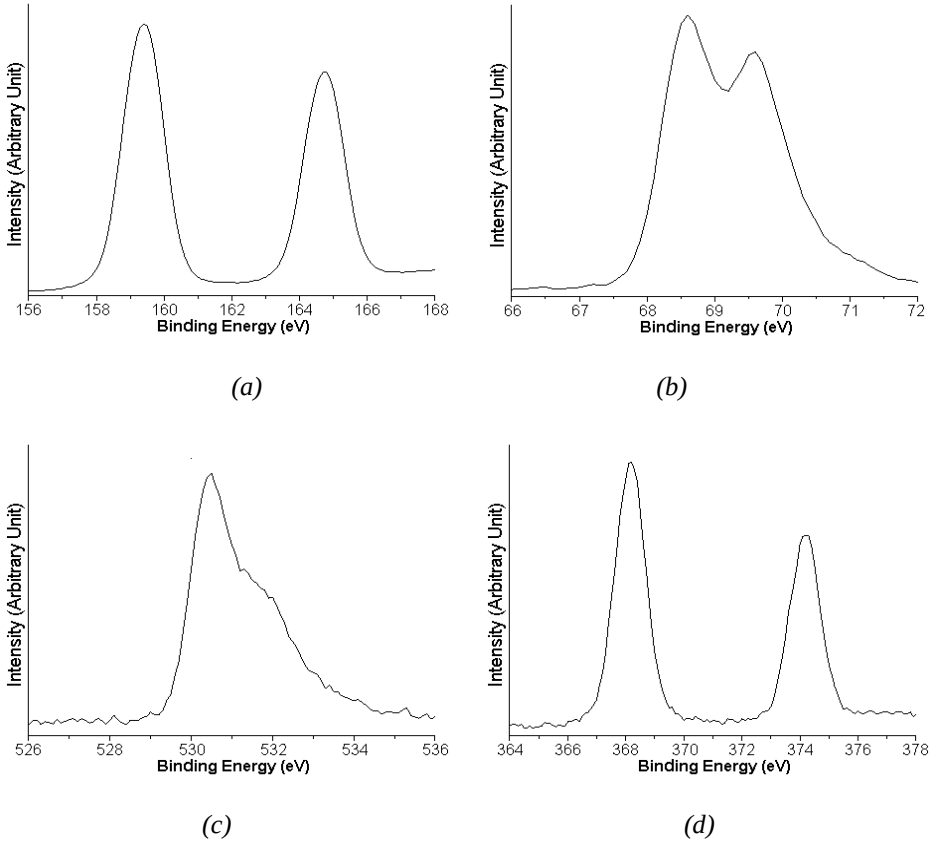

Fig. 3. XPS spectra of (a) Bi, (b) Br, (c) O and (d) Ag containing in 10 wt% Ag/BiOBr nanocomposites.

The photocatalytic activities of the heterostructure Ag/BiOBr nanocomposites were investigated for the degradation of MB under visible light irradiation as the results shown in Fig. 4a. It can be seen that the photolysis of MB was negligible under visible light illumination within 300 min. The photocatalytic efficiency for photodegradation of MB by pure BiOBr as the photocatalyst was 61 % under visible light irradiation. When Ag/BiOBr nanocomposites were introduced, the photocatalytic efficiencies were significant improved comparing with that of the pure BiOBr. Thus the Ag content had significant influence on the activity of Ag/BiOBr composites. Upon increasing the Ag content from 1 to 10 wt%, the photocatalytic efficiency for photodegradation of MB was almost 100 % by 10 wt% Ag/BiOBr under visible light illumination.

The kinetic reaction for photodegradation of MB by a photocatalyst was calculated through the pseudo-first-order kinetics by the below equation.

$$\ln(C_t/C_o) = -kt \quad (2)$$

, where C_t is the concentration of MB at time t, C_o is the concentration of MB at the establishment of adsorption/desorption equilibrium, and *k* is a kinetic constant [12, 13]. The k values for all the nanocomposites were calculated via the first-order linear fit from the linear relationship between

$-\ln(C_t/C_0)$ and the irradiation time as the results shown in Fig. 4b. In this research, the *k* by BiOBr was 3.33 x 10^{-3} min^{-1} and that by 10 wt% Ag/BiOBr was 0.0108 min^{-1} or 3.25 times of that of pure BiOBr. The stability of 10 wt% Ag/BiOBr nanocomposites was also investigated as the results shown in Fig. 4c. Clearly, the photocatalytic efficiency exhibited only a slight loss after the end of the fifth recycle, indicating that the photocatalyst was stable for photodegradation of MB.

The photocatalytic process over Ag/BiOBr nanocomposites under visible light irradiation can be explained by the following suggested mechanism shown in Fig. 4d. Under visible light irradiation, the photoinduced electron–hole pairs were generated in conduction and valence bands of BiOBr [6]. The photo-induced electrons diffused from BiOBr conduction band to Ag nanoparticles. Subsequently, the photo-induced electrons on Ag nanoparticles were scavenged by adsorbed oxygen molecules to form superoxide radical anions [2, 8]. Concurrently, holes in valence band were scavenged by OH^- to produce active radicals. Thus they can attack the MB molecules by transforming the MB molecules into H_2O and CO_2 as the final products [2].

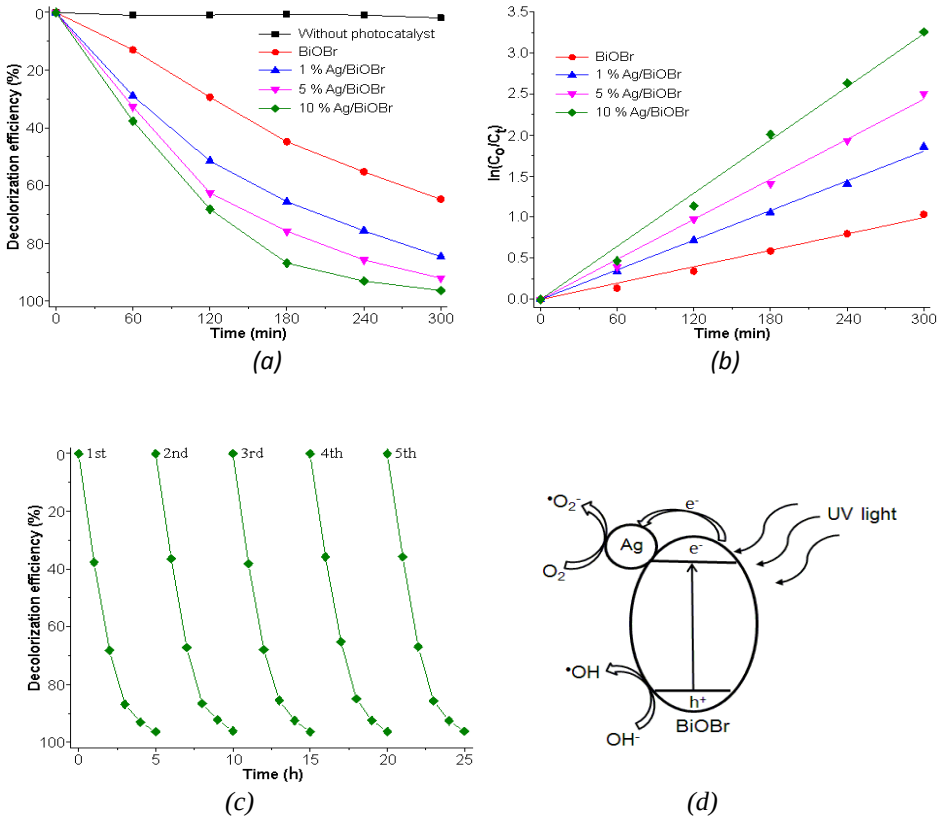

Fig. 4. (a) Decolorization efficiency and (b) first-order plot for photocatalytic degradation of MB by 0–10 wt% Ag/BiOBr samples under UV light irradiation. (c) Recyclability of photocatalytic degradation of MB by 10 wt% Ag/BiOBr nanocomposites. (d) Schematic diagram of electron-hole separation for photocatalysis of Ag/BiOBr nanocomposites.

4. Conclusions

Ag nanoparticles deposited on BiOBr nanoplates were successfully synthesized in this research. The Ag/BiOBr nanocomposites showed higher efficient activity for photodegradation of MB under UV light irradiation than the pure BiOBr nanoplates because Ag nanoparticles acted as reservoirs for photogenerated electrons, promoting the interfacial electron diffusion process between Ag nanoparticles and BiOBr nanoplates and facilitating the photocatalytic reaction of 10 wt% Ag/BiOBr nanocomposites to reach at the highest photocatalytic activity.

Acknowledgements

We are extremely grateful to Prince of Songkla University, Hat Yai, Songkhla 90112, Thailand for providing financial support the contact no. SCI620121S.

References

[1] T. Jiang, J. Li, Z. Sun, X. Liu, T. Lu, L. Pan, Ceram. Inter. **42**, 16463 (2016).
[2] A. Phuruangrat, S. Putdum, P. Dumrongrojthanath, N. Ekthammathat, S. Thongtem, T. Thongtem, Mater. Sci. Semicond. Process. **34**, 175 (2015).
[3] P. Patiphatpanya, A. Phuruangrat, S. Thongtem, T. Thongtem, Mater. Lett. **209**, 264 (2017).
[4] R. Li, X. Gao, C. Fan, X. Zhang, Y. Wang, Y. Wang, Appl. Surf. Sci. **355**, 1075 (2015).
[5] X. Xiong, L. Ding, Q. Wang, Y. Li, Q. Jiang, J. Hu, Appl. Catal. B **188**, 283 (2016).
[6] X. Zou, Y. Dong, X. Zhang, Y. Cui, X. Ou, X. Qi, Appl. Surf. Sci. **391**, 525 (2017).
[7] W. Guo, Q. Qin, L. Geng, D. Wang, Y. Guo, Y. Yang, J. Hazard. Mater. **308**, 374 (2016).
[8] B. Pant, M. Park, H.Y. Kim, S.J. Park, Synthetic Metal. **220**, 533 (2016).
[9] Powder Diffraction File, JCPDS-ICDD, 12 Campus Bld, Newtown Sq, PA 19073-3273, USA, 2001.
[10] J. Zhang, Z. Ma, Molecular Catal. **436**, 190 (2017).
[11] Z. Han, L. Ren, Z. Cui, C. Chen, H. Pan, J. Chen, Appl. Catal. B **126**, 298 (2012).
[12] B. Song, Q. Tang, Q. Li, W. Wu, H.L. Zhang, J. Cao, M. Ma, Mater. Lett. **209**, 251(2017).
[13] F. Zhang, T. Ding, Y. Zhang, Z. Yang, H. Xue, Mater. Lett. **192**, 149 (2017).